Environmental and
Biogeochemical Processes

https://doi.org/10.48130/ebp-0026-0016

Perspective

Open Access

An iron-centric framework for tracking redox biogeochemistry in paddy soils

Qianrui Huangfu[1,2], Luoqin Shen[1,3], Bang Ni[1,2], Shuai Du[1,2] and Sha Zhang[1,2*]

Received: 21 June 2026

Revised: 19 August 2026

Accepted: 17 September 2026

Published online: 19 October 2026

Abstract

Flooded paddy soils often experience a sustained iron (Fe) reduction window because reactive ferric Fe(III) minerals can persist through seasonal inundation rather than being completely exhausted. Within this window, reduction of Fe(III) to ferrous Fe(II) links anaerobic electron transfer to the cycling of carbon, nutrients, sulfur, and arsenic. Monitoring these transitions requires indicators that combine mechanistic relevance with field feasibility and reproducibility. Here, we propose an Fe-centric framework using total dissolved Fe (TDFe) as a process window indicator. Under typical circumneutral paddy conditions, the contrasting solubility behavior of Fe(III) and Fe(II) constrains dissolved Fe dynamics such that increases in TDFe primarily reflect Fe(II) accumulation during Fe(III) reduction. Acid fixation preserves dissolved Fe signals during sampling and storage, enabling reproducible tracking of the Fe reduction window. Coupled dissolved arsenic dynamics provide environmentally relevant corroboration that this window corresponds to reductive mobilization processes driven by Fe transformation. The redox interpretation of TDFe weakens where sulfide scavenges dissolved Fe; reactive Fe(III) minerals are limited, or Fe reduction becomes decoupled from dissolved Fe accumulation, requiring complementary redox potential, Fe speciation, or mineralogical analyses. Integrating TDFe with low-disturbance depth-resolved sampling (e.g., microdialysis profiles) could extend redox monitoring from bulk seasonal trends toward spatially resolved process dynamics. More broadly, this framework illustrates how chemically constrained process windows can transform complex redox transitions into measurable and management-relevant indicators.

Keywords: Soil redox, Spatiotemporal dynamics, Microdialysis, Dissolved iron, Iron speciation, Arsenic, Paddy soils

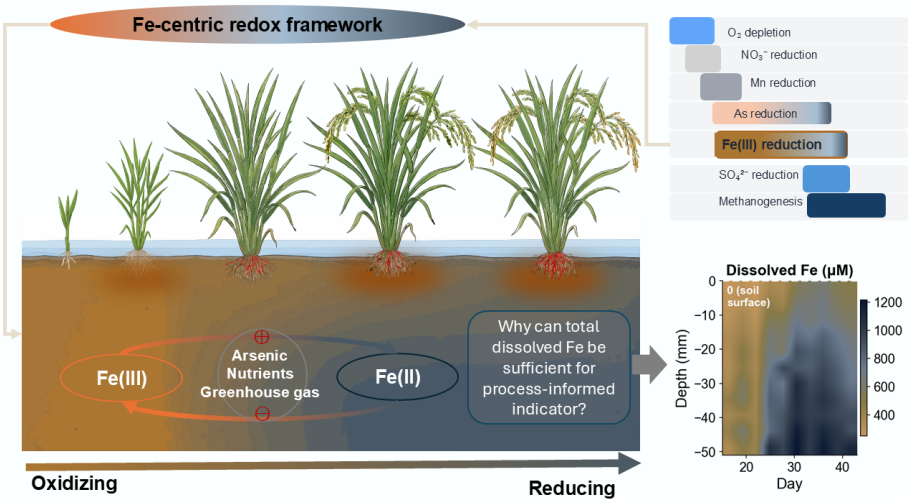
Highlights

- Total dissolved Fe effectively represents the reduced Fe pool.
- Total dissolved Fe tracks seasonal Fe reduction in freshwater paddies.
- Acid-fixed total Fe is reproducible for routine seasonal redox monitoring.
- Dissolved As complements Fe but does not replace As speciation.
- The indicator fails where sulfide scavenges dissolved iron.

* Correspondence: Sha Zhang (biogeochemx@outlook.com or szhang@iue.ac.cn)
Full list of author information is available at the end of the article.

https://doi.org/10.48130/ebp-0026-0016

Graphical abstract



Introduction

Soil and sediment redox conditions regulate a wide range of key biogeochemical processes, including greenhouse gas (GHG) emissions[1–3], nutrient transformations, and contaminant mobilization[2,4,5]. However, translating these dynamic processes into reliable indicators that are suitable for field monitoring at the seasonal scale remains challenging. In flooded agricultural systems, redox transitions occur continuously across spatial and temporal scales, and management decisions often require determining when reducing conditions develop, how long they persist, and where they occur[5–12].

The difficulty of redox monitoring arises from the complex and overlapping nature of reduction processes in soils. Although thermodynamic theory predicts a general sequence of electron acceptor utilization, including oxygen (O_2), nitrate, manganese, Fe(III) (hydr)oxides, sulfate, and carbon dioxide[13], flooded soils commonly exhibit concurrent redox reactions because of kinetic limitations, mineral heterogeneity, microbial interactions, and microscale environmental variability (Fig. 1)[3,12,14]. Consequently, approaches designed to resolve individual reactions or chemical species often require intensive sampling, careful sample preservation, and sophisticated analytical procedures, limiting their applicability for field-scale and seasonal monitoring programs[10,12,15]. This distinction highlights a fundamental difference between mechanistic characterization and operational monitoring: although detailed measurements may identify specific reactions, field monitoring requires indicators that capture environmentally meaningful process transitions with sufficient reproducibility.

Such indicators should track a process that is both environmentally consequential and capable of producing an abundant and measurable signal. Among the major electron acceptors involved in flooded soil-related reduction, iron (Fe) uniquely satisfies these requirements[5,13]. Agricultural soils commonly contain approximately 2%–4% total Fe by weight, predominantly in silicate minerals and Fe (hydr)oxides, a concentration comparable in magnitude to soil organic matter content[16,17]. Iron (hydr)oxides represent a major electron-accepting pool during soil reduction, and the transformation between ferric Fe(III) and ferrous Fe(II) constitutes a key transition within paddy redox sequences[4,14,16,17]. Fe(III) reduction occurs across a broad range of environmentally relevant reducing conditions and intersects with redox transitions involving manganese and sulfur, allowing Fe cycling to link multiple coupled biogeochemical processes (Fig. 1a)[5,13,14]. Because reactive Fe(III) minerals are abundant and often persist through seasonal flooding cycles, Fe(III) reduction can represent a sustained redox window rather than a transient transition during soil reduction[12,18]. Critically, Fe transformation couples a large solid-phase reservoir with a measurable dissolved-phase response, providing an operational signal that links redox processes with field-observable chemical changes[5]. Through these transformations, Fe cycling influences multiple coupled processes, including methane production and emissions, the availability of nitrogen (N) and phosphorus (P), and the mobility of redox-sensitive metal(loid)s, especially arsenic (As) and cadmium (Cd) (Fig. 1b)[4,7,19–23].

In paddy ecosystems, periodic flooding–drainage cycles repeatedly drive Fe(III) reduction and Fe(II) oxidation, generating seasonal changes in Fe mineral phases and dissolved Fe distributions across the soil–water interface (SWI) and the rhizosphere (Fig. 1c–e)[5,18,20,24]. Such demonstrations suggest that the transformation of Fe may provide a process window for tracking broader redox transitions[14]. During reduction, progressive changes in Fe mineral phases across the SWI reflect reductive dissolution, whereas the intrusion of oxygen (O_2) promotes Fe(II) oxidation and Fe plaque formation in the rhizosphere (Fig. 1c, d). Moreover, depth-resolved observations of the distributions of dissolved Fe and As demonstrate pronounced spatial and temporal heterogeneity associated with Fe-mediated redox processes at the SWI (Fig. 1e)[18].

Characterizing these redox transitions in field environments relies on a range of established approaches, each with distinct trade-offs between mechanistic resolution, analytical complexity, and field applicability (Fig. 2). These approaches include redox potential (Eh), porewater sampling techniques such as Rhizon samplers[25], high-resolution peepers (HR-Peeper), O_2-free microdialysis profilers[26], and diffusive gradients in thin films (DGTs)[27,28], as well as complementary analytical platforms including electrochemical sensing[29], spectroscopy[30], mass spectrometry (MS), and ion chromatography (IC) (Fig. 2). Among these methods, Eh is widely applied because of its operational simplicity, but it is not process-specific and is constrained by poor reproducibility and qualitative

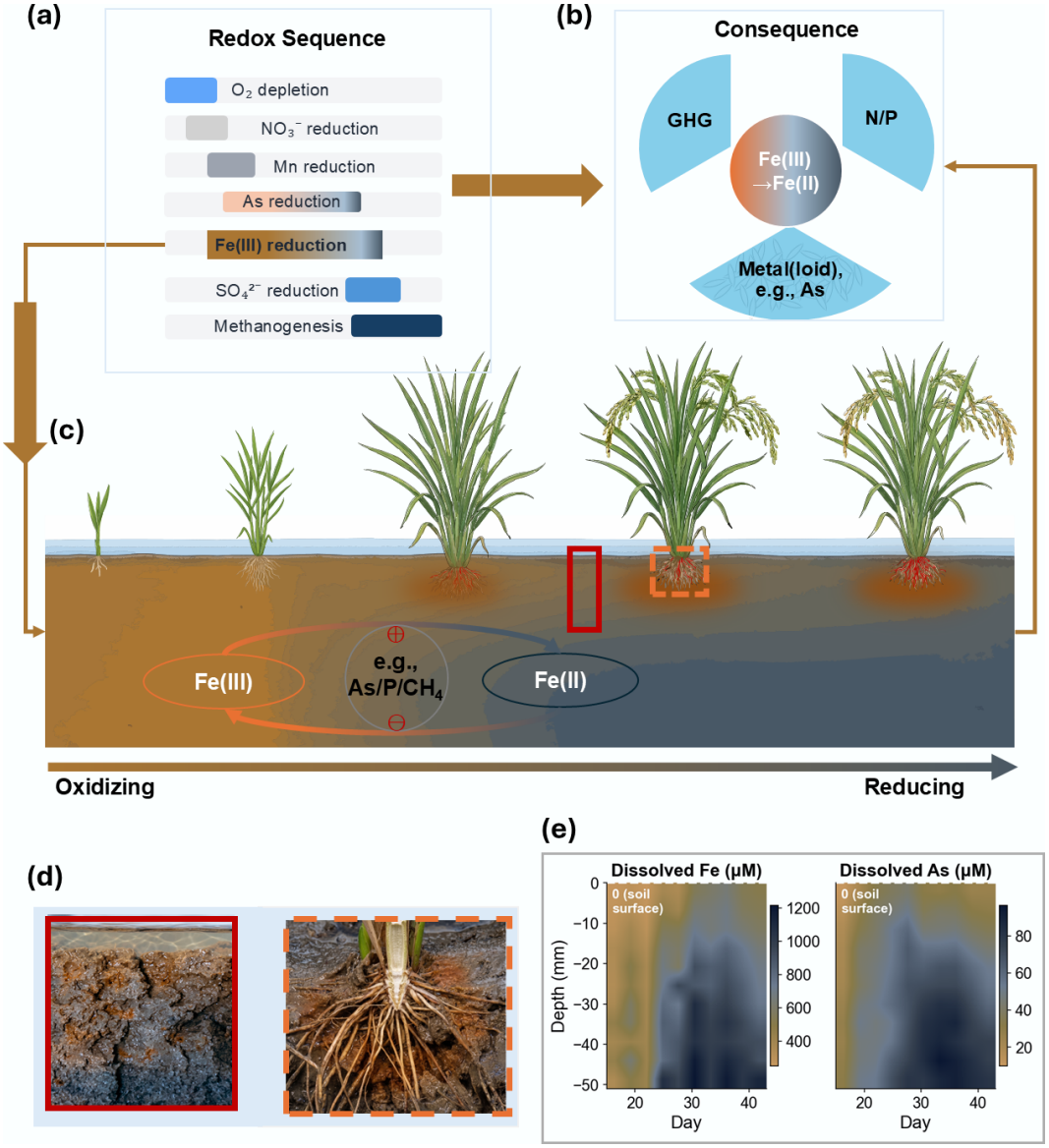


Fig. 1 Iron cycling as a redox hub linking greenhouse gas (GHG) emissions, nutrient availability, and metal(loid) dynamics in paddy soils. (**a**) Thermodynamically constrained redox succession of major electron acceptors during soil-based reduction. (**b**) Iron cycling functions as a biogeochemical control point regulating GHG emissions, nutrient transformations (e.g., N and P), and metal(loid) mobility, particularly As. (**c**) Progressive color transitions across the soil–water interface (SWI) reflect Fe mineral transformation during reduction, whereas the rust-colored rhizosphere indicates the formation of Fe plaques through oxygen-mediated oxidation of ferrous Fe(II). (**d**) Photographs illustrating spatial variations in iron-associated color development across the SWI and the rhizosphere. (**e**) Spatiotemporal distributions of dissolved Fe and As at the SWI during flooding, reconstructed from replicate-averaged concentrations reported in a previous study (note that depth-resolved pH ranges from 3.42 to 6.07)[18].

interpretations[29,31]. Other approaches provide quantitative chemical information but are often restricted to particular species or require specialized analytical workflows. Therefore, obtaining a comprehensive understanding of the soil's reduction processes frequently requires researchers to combine multiple techniques, introducing substantial operational challenges for routine monitoring programs.

Several Fe-based indicators have demonstrated that Fe transformation can visually indicate reducing conditions in field environments. For example, the Soil Reduction Indicator (IRIS) uses plastic plates coated with Fe paints to record the reduction process by the degree of Fe (hydr)oxide removal (Fig. 2a bottom left)[6,9,15,32–34]; the Fe/steel rod method uses changes in the (hydr)oxide film on the Fe surface to reflect long-term exposure to reduction (Fig. 2a bottom left)[8,35]. These methods demonstrate the value of Fe transformation as an indicator of soil reduction but primarily reflect changes in solid-phase Fe materials; these methods face difficulties in redox-relevant quantification and cannot directly provide dissolved-phase signals that are compatible with conventional chemical monitoring[2,15,21,22,36]. Recent developments in low-disturbance sampling, including temporally and spatially resolved microdialysis profiling, demonstrated the feasibility of tracking the dynamics of total dissolved Fe (TDFe) and other redox-sensitive solutes simultaneously across incubation time and the SWI[18,26]. However, whether TDFe pools can provide a stable and reproducible signal suitable for season-scale redox monitoring remains unresolved.

https://doi.org/10.48130/ebp-0026-0016

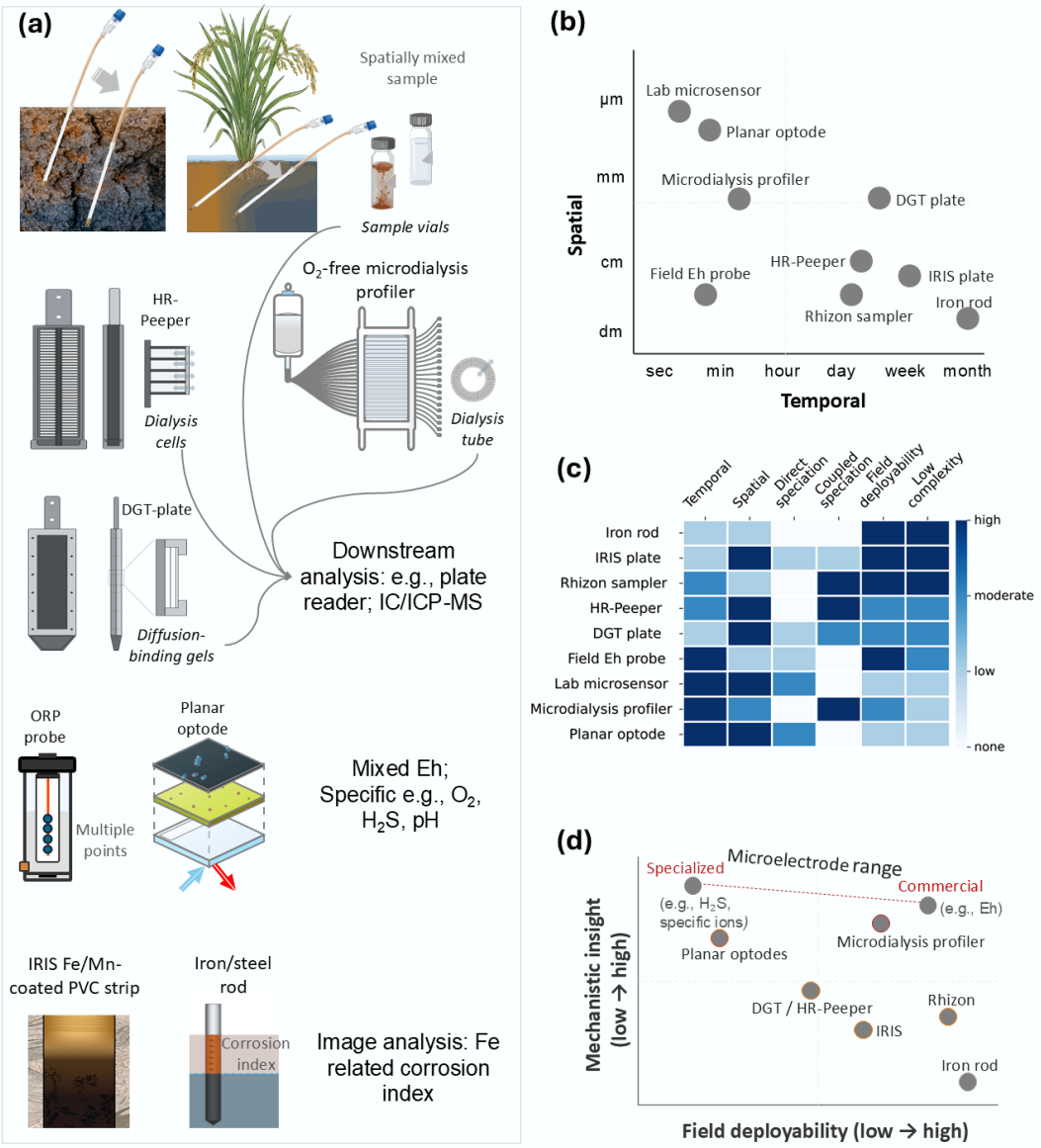


Fig. 2 Methods for tracking redox dynamics in paddy soils. (**a**) Overview of representative approaches, including porewater samplers (Rhizon, HR-Peeper, and O_2-free microdialysis profilers), DGT-based chemical imaging, direct sensors (oxidation–reduction potential [ORP or Eh] probes and planar optodes), and Fe-based indicators (IRIS and Fe/steel rods). Chemical speciation from sampling-based approaches generally requires coupling with complementary techniques (e.g., spectroscopy, IC, or inductively coupled plasma – mass spectroscopy [ICP-MS]). (**b**) Comparison of the spatial and temporal resolution domains covered by different approaches. (**c**) Relative evaluation of analytical capabilities, including spatiotemporal resolution, speciation potential, field deployability, and technical complexity. (**d**) Conceptual trade-off between process interpretation potential and field applicability.

This perspective addresses the unresolved challenge of translating Fe-mediated reduction into a practical, process-informed monitoring signal. We develop an Fe-centric framework in which TDFe is evaluated as a potential process window indicator rather than as a universal measure of soil redox status. We first establish the chemical basis for interpreting acid-fixed TDFe under circumneutral paddy conditions, and then examine its value relative to established redox and Fe-speciation approaches. We next use coupled Fe–As behavior as an environmentally relevant line of evidence for evaluating whether TDFe tracks Fe-mediated reduction, before defining the environmental and temporal conditions that constrain this interpretation. Finally, we consider how TDFe trajectories could be integrated with complementary measurements and future process-based models to support the monitoring and management of redox-sensitive environmental processes. This framework shifts the emphasis from identifying a single universal redox indicator toward defining when a measurable chemical signal remains mechanistically interpretable and operationally useful.

Key basis for the Fe-centric redox framework

From the thermodynamic and biogeochemical perspectives, Fe(III) reduction represents a critical transition and generally occurs after the depletion of higher-energy electron acceptors during the development of reducing conditions in flooded soils[11,12,37–40].

However, reactive Fe(III) reduction in flooded soils rarely proceeds through a strictly sequential pathway or results in complete depletion, because the reaction kinetics, mineral accessibility, and microscale heterogeneity sustain overlapping redox processes across spatially and temporally heterogeneous environments (see the examples of rust patches and concentration hotspots in Fig. 1d, e)[6,11,12,17,41]. This fact likely puts the paddy's biogeochemistry into the window between Fe(III) reduction and Fe(II) oxidation processes. In particularly, the redox potentials of the Fe(III)–Fe(II) couple are positioned between those of other major key redox couples ranging from O_2 consumption to methanogenesis[13,14,42–45]. Consequently, Fe transformation influences multiple ecosystem processes. Iron (hydr)oxides serve as major reservoirs for As and P, and their reductive dissolution can alter the mobility and bioavailability of these elements[11,42–44,46]. Meanwhile, Fe(III) reduction influences carbon cycling by competing with methanogenesis for electron donors such as acetate and hydrogen, thereby regulating GHG production under flooded conditions[37–41,45,47]. Experiments using Fe-containing amendments, such as Fe slag, have also demonstrated that Fe inputs can suppress methane and nitrous oxide emissions from paddy soils[44]. Importantly, the relevance of Fe as a redox indicator does not depend on the complete depletion of primary Fe(III) minerals. In natural paddy systems, secondary reactive Fe(III) phases can also be regenerated through repeated flooding–drainage cycles[5,12]. This persistence allows Fe transformation to provide a recurring observation window for seasonal redox transitions rather than representing a one-time depletion process. This principle has been empirically validated by, as mentioned earlier, the IRIS and Fe/steel rod methods (Fig. 2)[6,9,15,32–35]; spatially heterogeneous patches are created on the Fe(III) films and the Fe rod's surfaces along the SWI redox gradient.

From mechanistic measurements to operational redox indicators

Environmental redox monitoring requires a balance between mechanistic resolution and operational feasibility. Indicators that directly resolve specific redox reactions often provide strong information on the process but may be difficult to apply consistently across field settings, whereas integrative measurements improve comparability at the expense of process specificity[20,48,49]. Conventional approaches therefore differ in their ability to translate redox processes into reproducible monitoring signals, depending on whether they capture bulk redox conditions, specific Fe transformations, or integrated dissolved-phase responses (Fig. 2).

Oxidation–reduction potential probes for measuring Eh remain a preferred method, and these provide a rapid measurement of the overall tendency of a submerged system toward oxidation or reduction[31,50]. However, this integrative characteristic also limits its process-informed interpretations. In flooded soils, Eh reads represent a mixed potential generated by multiple redox couples under nonequilibrium conditions rather than the equilibrium potential of a single reaction system[10,15,50,51]. In addition, measured Eh values are strongly influenced by the electrode's surface conditions, selection of the reference electrode, equilibration time, and measurement procedures[50–53]. Differences among instruments and operators can therefore introduce substantial variability, particularly in strongly reducing environments where stable readings may require prolonged equilibration periods[50,53,54].

Direct measurements of Fe speciation provide more direct information on Fe transformation than Eh measurements because Fe(II) and Fe(III) concentrations and their ratios provide information on the extent of Fe(III) reduction[55]. They remain indispensable for mechanistic studies requiring molecular-level chemical resolution, including reaction mechanisms, toxicity pathways, and mineral interactions[55,56]. However, their application in field monitoring is constrained by the instability of reduced Fe(II) species during sampling and preservation[57,58]. Dissolved Fe(II) can be rapidly oxidized upon exposure to O_2, and its oxidation kinetics are strongly dependent on the pH, dissolved oxygen concentration, and ligand conditions[58–61]. Under oxygenated conditions, substantial Fe(II) transformation may occur within typical sample handling periods, causing measured Fe(II)/Fe(III) ratios to partially reflect sampling artifacts rather than *in situ* conditions[59–62]. Although anoxic sampling and preservation procedures improve reliability, they remain difficult to implement at the spatial and temporal scales required for routine field monitoring[57,63,64].

These limitations highlight the need for indicators that retain a mechanistic linkage with Fe-mediated reduction while providing sufficient reproducibility for field-scale comparisons. TDFe represents one such operational approach because it integrates dissolved Fe measurements without requiring the separation of individual Fe species during routine analysis. Acid-preserved TDFe can be determined using established colorimetric or spectroscopic methods that are routinely applied in soil and water analyses. Because TDFe integrates dissolved Fe species after preservation, it may provide a more reproducible operational signal than individually resolved Fe species when routine monitoring prioritizes comparability across samples and time points[57]. High-resolution investigations have shown that total elemental pools can display greater spatial stability than highly reactive or fractionated pools, supporting the use of total dissolved concentrations for monitoring applications where reproducibility is prioritized[65]. Accordingly, TDFe provides a process-oriented indicator that complements rather than replaces Eh and Fe speciation approaches. When combined with complementary process measurements, TDFe's dynamics can provide additional context for interpreting environmentally relevant redox transformations[22,23,66,67]. The chemical basis underlying this interpretation and the environmental boundaries of TDFe's applicability are discussed in the following section.

Chemical basis and applicability boundaries of TDFe as a redox indicator

Interpreting TDFe as a redox indicator requires us to distinguish between measuring a chemical pool and identifying a biogeochemical process. The dissolved Fe concentration alone does not directly represent soil reduction because aqueous Fe is regulated by multiple coupled processes, including Fe(III) mineral reduction, dissolution, retention, precipitation, and reoxidation[4,13,68]. Therefore, TDFe becomes informative only when these processes remain coupled within an environmental window where Fe reduction generates a measurable dissolved Fe response.

The chemical basis of this interpretation follows from the contrasting behavior of Fe(III) and Fe(II). Agricultural soils contain substantial Fe(III) reservoirs, primarily associated with Fe (hydr)oxides, including ferrihydrite, goethite, and other poorly crystalline phases. Under circumneutral conditions, these Fe(III)-bearing minerals exhibit low solubility, and inorganic dissolved Fe(III) concentrations reach a minimum near pH 7–8, with reported concentrations approaching approximately 0.01 nM (Fig. 3)[69–71]. During prolonged flooding, oxygen and other high-potential electron acceptors are progressively depleted, promoting the

https://doi.org/10.48130/ebp-0026-0016

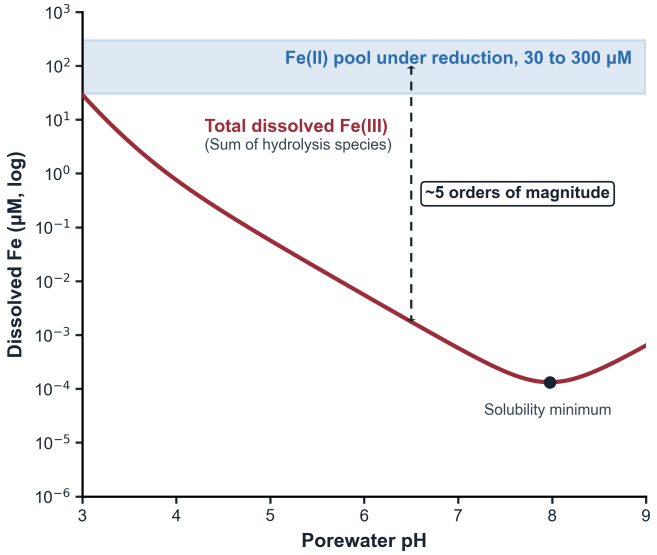


Fig. 3 Thermodynamic and kinetic basis for TDFe's accumulation under flooded paddy conditions. The red curve represents the theoretical upper constraint of dissolved inorganic Fe(III) concentrations imposed by ferric hydroxide's solubility across pH gradients (calculated from cumulative hydrolysis equilibria). The blue region represents the expected dissolved Fe(II) accumulation range under reducing paddy conditions based on reaction–transport simulations and independent field observations, assuming typical paddy parameters (reduction intensity $r \in [0.05, 1]$, sulfate 0–100 μM). All hydrolysis constants are derived from Stefánsson[69]. The range of 30–300 μM fpr porewater Fe(II) under reducing conditions was obtained from independent field observations by Weber et al.[75] and Roberts et al.[63].

microbial reduction of Fe(III)-bearing minerals[37,72–74]. This process transfers Fe from relatively immobile solid-phase reservoirs into the aqueous phase as Fe(II). Because Fe(II) is substantially more soluble than Fe(III) under reducing conditions, dissolved Fe can accumulate when Fe(II) production exceeds its removal through secondary processes, resulting in porewater Fe concentrations ranging from tens to hundreds of micromolar in freshwater paddy soils[63,75] (Fig. 3).

Consequently, under the circumneutral flooded paddy conditions considered here, increasing TDFe primarily reflects the progressive mobilization of Fe from solid-phase Fe(III) reservoirs into the dissolved Fe pool. Importantly, TDFe should not be interpreted as a direct measurement of the intensity of reduction. Instead, it represents the integrated chemical response produced by Fe reduction and subsequent Fe(II) accumulation over a defined temporal window. High TDFe indicates that Fe reduction has proceeded sufficiently for dissolved Fe to accumulate, but does not necessarily indicate that the entire soil is more strongly reduced than a soil with lower TDFe. Conversely, low TDFe does not necessarily indicate oxidizing conditions because dissolved Fe accumulation may be limited by insufficient reactive Fe supply, rapid Fe removal, or competition from alternative electron acceptors. Thus, TDFe provides information on the development and persistence of Fe-mediated reduction rather than on a universal ranking of soil redox strength. However, the relationship between TDFe accumulation and Fe reduction is conditional because dissolved Fe concentrations are controlled by concurrent production and removal processes. The environmental conditions defining this coupling and the resulting applicability domain of TDFe are discussed in the following section.

Coupled Fe and As redox behaviors validate environmental relevance of the TDFe indicator

Using TDFe as a process-window indicator can lead to environmentally relevant consequences. Mobilization of As provides an intricate validation framework because the behavior of As in freshwater paddy soils is strongly regulated by Fe's mineral dynamics, with Fe reduction acting as the major driver of the release and redistribution of As[66,67,76]. In flooded paddy soils, As is strongly associated with Fe(III) mineral surfaces through adsorption and co-precipitation processes, particularly with short-range-order Fe oxides that provide abundant reactive surface sites[42,76–78]. When microbial reduction destabilizes Fe(III)-bearing minerals during prolonged flooding, previously associated As can be released into the porewater, resulting in the enhanced mobility and bioavailability of As[21,22,66,79]. Field incubation studies have shown that dissolved Fe and As often increase concurrently as Eh declines toward the Fe-reduction transition zone, with both elements beginning to mobilize at around approximately +100 mV under relevant conditions[75,80]. High-resolution rhizosphere measurements also demonstrated that Fe and As fluxes can spatially co-localize in the rhizosphere, supporting their mechanistic linkage during redox-driven mineral transformation[81].

However, the Fe–As coupling is not a simple, one-to-one relationship. Dissolved As concentrations are also controlled by As speciation, readsorption, secondary mineral formation, organic matter interactions, and sulfide-driven transformations[22,78,79,82]. For example, secondary Fe mineral formation can cause partial As immobilization through sulfide precipitation, whereas thiolation of As can also mobilize As[22,82,83]. At extreme conditions, the dissolved As concentration cannot serve as a direct surrogate for the intensity of Fe(III) reduction (see the further discussions in the following section). In most cases, the value of Fe–As coupling lies in demonstrating its environmental relevance, which has been extensively validated[67,22,84]. When increasing TDFe coincides with increasing dissolved As, this coordinated response indicates that Fe reduction has progressed sufficiently to produce both an aqueous Fe signal and an environmentally meaningful consequence. In this context, TDFe identifies the Fe(III)-mediated reduction process, whereas As provides evidence that this process influences contaminants' mobility.

The strength of the Fe–As coupling remains context-dependent. In paddy soils, reductive Fe(III) dissolution and As mobilization often form a connected process sequence, so that TDFe indicates a transition linked to contaminant release. In settings where sulfide control, external As inputs, or extensive secondary mineral stabilization predominate, this relationship weakens and additional measurements are required[79]. When the objectives include assessing As toxicity, plant uptake, or long-term transport, speciation of arsenite, arsenate, and methylated As remains essential because total dissolved As concentrations alone do not resolve these pathways[4,85].

Applicability domain of TDFe-based redox monitoring

Defining the applicability domain is essential for determining when TDFe can serve as a meaningful indicator of Fe-mediated reduction. We applied a simplified zero-dimensional mass-balance framework inspired by early diagenetic modeling approaches[74,86,87]. This

framework is not intended as a predictive model or quantitative calibration tool, but rather as an order-of-magnitude analysis to illustrate the conditions under which dissolved Fe accumulation remains coupled with Fe reduction. The applicability of TDFe therefore depends on the processes controlling Fe dissolution and removal[66,22,88,89].

The TDFe framework is most applicable in freshwater paddy soils where three conditions are simultaneously satisfied: (i) sufficient reactive Fe(III)-bearing minerals are available as electron acceptors, (ii) prolonged flooding promotes anaerobic Fe reduction, and (iii) dissolved Fe accumulation is not rapidly offset by competing removal processes (Fig. 4). Under these conditions, increases in TDFe primarily reflect the transformation of relatively immobile Fe(III)-bearing solids into a more mobile dissolved Fe(II) pool, providing an operational window for tracking Fe-mediated reduction. However, this relationship is conditional because dissolved Fe concentrations represent the net balance between Fe mobilization and subsequent retention or removal processes.

Several environmental factors can weaken this relationship (referred to as decoupling) and constrain the interpretation of TDFe. First, the availability and mineralogical characteristics of the Fe phases determine whether microbial Fe reduction can generate a measurable dissolved Fe response. Soils dominated by poorly reducible crystalline Fe minerals, structurally incorporated Fe, or limited reactive Fe pools may undergo anaerobic Fe transformation without substantial increases in TDFe[88,90]. In such systems, low TDFe does not necessarily indicate weak reducing conditions but may instead reflect limited Fe availability or restricted Fe mobilization. Second, the chemical conditions controlling dissolved Fe retention provide another major constraint. Strong sulfide production can promote the formation of Fe sulfide and reduce TDFe concentrations despite ongoing Fe reduction[91,92]. As sulfate's availability increases, sulfide production may remove Fe(II) through precipitation of Fe sulfide faster than reductive dissolution can replenish dissolved Fe, resulting in declining or stabilized TDFe despite increasingly reducing conditions (Fig. 4). This transition depends on interacting controls, including the sulfate supply, organic carbon availability, the abundance of reactive Fe, and the sulfate reduction kinetics[64,91,93]. However, because sulfate availability is generally limited in many freshwater paddy systems, and because alternative electron acceptors may delay the progression of sulfate reduction pathways, sulfide-induced decoupling is often constrained and may primarily attenuate rather than completely reverse the TDFe response[37,82,94].

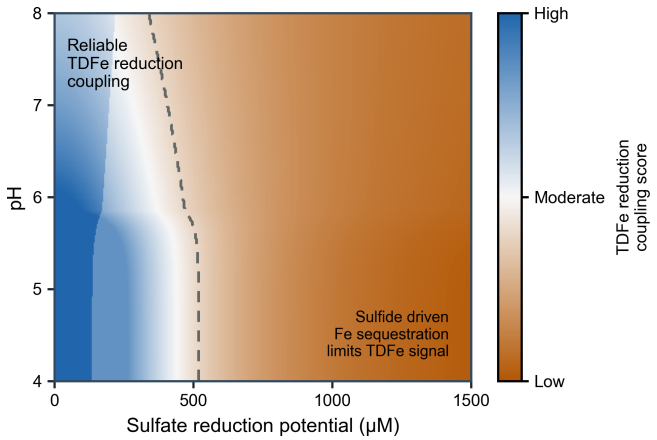


Fig. 4 Conceptual applicability domain of TDFe as a process-window indicator of Fe reduction, shown as a reaction–transport-based evaluation of TDFe–reduction coupling across sulfate reduction potential and pH gradients. Blue regions represent conditions where dissolved Fe provides a monotonic and sensitive signal of Fe reduction, whereas orange regions indicate decoupling caused by competing Fe sequestration or limited accumulation of dissolved Fe. The transition zone is conditional on reactive Fe's availability, the organic carbon supply, and the sulfate reduction kinetics rather than being defined by a universal threshold.

Other geochemical conditions may also modify the relationship between TDFe and Fe reduction. For example, strongly acidic environments can increase ferric mineral dissolution and weaken the assumption that the accumulation of dissolved Fe primarily reflects reductive Fe mobilization (Fig. 3)[68,95,96]. Conversely, ligand-rich environments may enhance dissolved Fe concentrations through complexation processes that are independent of Fe reduction intensity[68,95]. These conditions illustrate that TDFe should be interpreted as a process-linked indicator only when Fe reduction remains the dominant control on the accumulation of dissolved Fe.

Hydrological transitions further define the temporal resolution at which TDFe can be meaningfully interpreted. Because dissolved Fe integrates mineral dissolution, microbial reduction, and secondary transformation processes, TDFe represents a process trajectory rather than an instantaneous redox state. During flooding–drainage transitions, dissolved Fe concentrations may lag behind the underlying redox changes because Fe oxidation, mineral transformation, and renewed dissolution are not instantaneous processes[59,22]. Such hysteresis limits the interpretation of TDFe as a direct indicator of short-term redox fluctuations but does not prevent its use for tracking broader seasonal reduction trajectories.

Spatial and temporal scales represent additional constraints on the interpretation of TDFe. Paddy soils contain strong microscale gradients of oxygen availability, microbial activity, mineral distribution, and elemental fluxes at the SWI and in the rhizosphere[74,86,87,97–99]. Because TDFe integrates dissolved Fe responses over broader spatial and temporal scales, it cannot resolve microscale variations in mineral phases, reactive Fe pools, or chemical speciation[65,74,86,87,97]. High-resolution approaches, including low-disturbance stratified sampling and microdialysis-based profiling, therefore remain essential for resolving fine-scale dissolved solute dynamics and mechanistic processes[26,84,100]. In addition, conventional filtration may retain or include colloidal Fe-bearing phases, meaning that operationally defined TDFe should be interpreted as a reproducible dissolved-phase signal rather than an absolute measure of all aqueous forms of Fe[64,82,92,93,101]. Therefore, TDFe is most appropriately interpreted as a seasonal or management-scale indicator of Fe-mediated reduction trajectories rather than as an instantaneous measure of microscale redox fluctuations.

Conclusion and outlook

The central contribution of this Perspective is the recognition that TDFe can serve as a process-window indicator within explicitly defined environmental boundaries. By integrating the transformation of Fe minerals, electron transfer processes, and measurements of the dissolved phase, TDFe provides an operational approach for tracking the progress of Fe-mediated reduction in freshwater paddy soils while avoiding several limitations. Within this framework, TDFe measurements bridge mechanistic understanding and environmental management. Temporal TDFe trajectories can complement targeted measurements of methane emissions, As behavior, and nutrient

https://doi.org/10.48130/ebp-0026-0016

dynamics by identifying periods when Fe-mediated processes are likely to influence carbon, contaminant, and nutrient cycling. Rather than replacing detailed chemical analyses, TDFe provides a scalable monitoring signal that can guide when and where higher-resolution measurements are most informative.

A major future direction is to move from interpreting TDFe as a descriptive indicator toward integrating TDFe trajectories into process-based predictive frameworks (Fig. 5). Coupling TDFe dynamics with carbon turnover, contaminant transport, and nutrient cycling models may transform dissolved Fe measurements into decision-support variables for adaptive water and fertilizer management. For instance, existing bottom-up approaches for estimating global methane emissions that emphasize carbon availability and environmental drivers often overlook the role of alternative electron acceptors, such as Fe(III), in controlling methanogenesis and emission dynamics[102]. A model that describes the relationship between porewater TDFe and methane emissions would provide an alternative approach for estimating methane emissions. Such developments require calibration across diverse soil types and hydrological regimes, together with an explicit consideration of the applicability boundaries identified in this perspective.

More broadly, this perspective highlights a shift from searching for universal redox indicators toward selecting process-linked indicators with defined domains of validity. The value of an environmental indicator lies not only in the magnitude of its signal but also in understanding the processes that generate that signal and the conditions under which it remains interpretable. Establishing such process-based frameworks will improve the transferability, reproducibility, and management relevance of redox monitoring across complex soil and aquatic environments.

Ethical statements

Not applicable. During the preparation of this work, the authors used Claude Opus 4.8 to polish the language and logic of the initial draft. All scientific content, data analysis, and interpretation were authored and verified by the authors. After using this tool the authors reviewed and

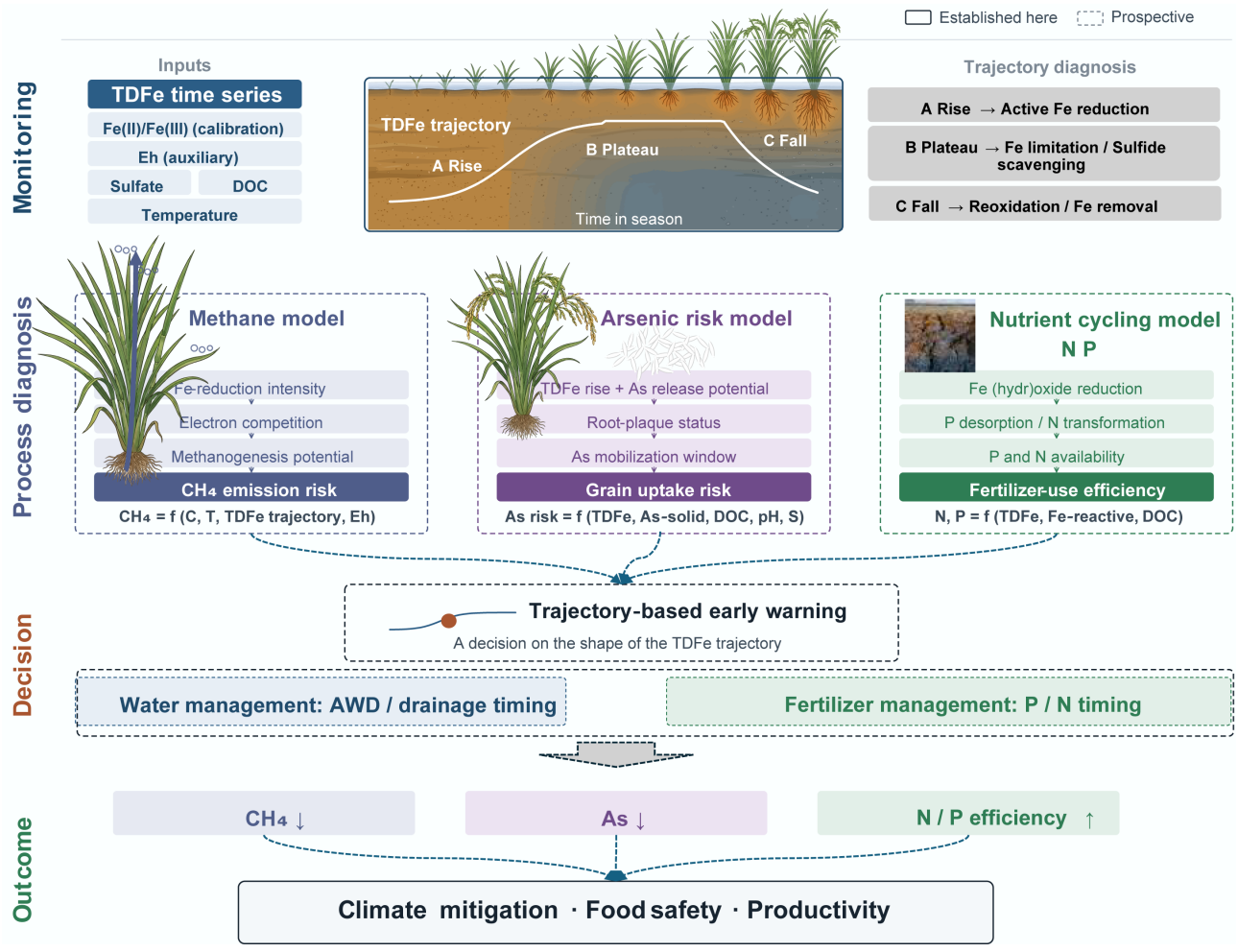


Fig. 5 From TDFe monitoring to process-informed environmental management in flooded soils. A prospective framework in which TDFe serves as a process variable rather than an endpoint measurement. A temporally resolved TDFe trajectory is interpreted to identify the distinct phases of Fe-mediated reduction dynamics, including increased accumulation of dissolved Fe, constrained Fe mobilization or sulfide-related attenuation, and oxidative recovery (Layer 1). These trajectories can inform coupled process models describing methane emissions, mobilization of As, and nutrient (e.g., N and P) dynamics (Layer 2), enabling trajectory-based early warning frameworks to support adaptive water and fertilizer management (Layer 3). The ultimate goal is to integrate redox process monitoring with climate mitigation, food safety, and nutrient use efficiency objectives (Layer 4). Solid outlines denote concepts established in this Perspective; dashed outlines indicate prospective developments. All trajectories are schematic.

edited the content as needed and take full responsibility for the content of the published article.

Author contributions

The authors confirm their contributions to this study as follows: Qianrui Huangfu: writing – original draft, writing – review and editing; Luoqin Shen: writing – review and editing; Bang Ni: writing – review and editing; Shuai Du: writing – review and editing; Sha Zhang: conceptualization, methodology, investigation, data curation, writing – original draft, writing – review and editing, supervision, funding acquisition. All authors reviewed the results and approved the final version of the manuscript.

Data availability

The model descriptions, parameters, data sources, and code used to generate Figs 1, 3, and 4 are available at https://github.com/biogeochemx/iron-centric-framework. The repository includes the Jupyter notebooks used for reproducing each figure, the input data for Fig. 1 (porewater Fe/As grids in data), and the pre-rendered figure outputs in the figures.

Acknowledgments

No acknowledgments are applicable for this work.

Funding

This work was financially supported by the National Key Research and Development Program of China (2023YFC3709100), the Fujian Provincial Science and Technology Program (2026R0102), and the Natural Science Foundation of Xiamen, China (3502Z202673062).

Declarations

Competing interests

The authors declare that they have no known competing financial interests or personal relationships that could have appeared to influence the work reported in this paper.

Author details

[1]State Key Laboratory of Regional and Urban Ecology, Ningbo Observation and Research Station, Institute of Urban Environment, Chinese Academy of Sciences, Xiamen 361021, China; [2]Zhejiang Key Laboratory of Urban Environmental Processes and Pollution Control, Chinese Academy of Sciences Haixi Industrial Technology Innovation Center in Beilun, Ningbo 315830, China; [3]College of Resources and Environment, University of Chinese Academy of Sciences, Beijing 100049, China

References

[1] Conrad R. 1996. Soil microorganisms as controllers of atmospheric trace gases (H_2, CO, CH_4, OCS, N_2O, and NO). *Microbiological Reviews* 60:609–640

[2] Saunois M, Martinez A, Poulter B, Zhang Z, Raymond PA, et al. 2025. Global methane budget 2000–2020. *Earth System Science Data* 17:1873–1958

[3] Grimm H, Drabesch S, Nicol A, Straub D, Joshi P, et al. 2024. Arsenic immobilization and greenhouse gas emission depend on quantity and frequency of nitrogen fertilization in paddy soil. *Heliyon* 10:e35706

[4] Chen N, Fu Q, Wu T, Cui P, Fang G, et al. 2021. Active iron phases regulate the abiotic transformation of organic carbon during redox fluctuation cycles of paddy soil. *Environmental Science & Technology* 55:14281–14293

[5] Zhang S, Zhu D. 2025. Microbial iron mining: a nature-based solution for pollution removal and resource recovery from contaminated soils. *Environmental and Biogeochemical Processes* 1:e006

[6] Dorau K, Zanger T, Bolten A, Mansfeldt T. 2024. Soil redox maps: assessment of small field-scale redox zonation by Mn and Fe oxide-coated IRIS films. *Journal of Soils and Sediments* 24:1206–1219

[7] Kögel-Knabner I, Amelung W, Cao Z, Fiedler S, Frenzel P, et al. 2010. Biogeochemistry of paddy soils. *Geoderma* 157:1–14

[8] Naveen S, Nair S, Velmurugan E. 2026. Soil redox micro-environments and paddy yield variation in Kole wetlands. *Madras Agricultural Journal* 113:221–227

[9] Sapkota Y, Duball C, Vaughan K, Rabenhorst MC, Berkowitz JF. 2022. Indicator of reduction in soil (IRIS) devices: a review. *Science of the Total Environment* 852:158419

[10] Tanji KK, Gao S, Scardaci SC, Chow AT. 2003. Characterizing redox status of paddy soils with incorporated rice straw. *Geoderma* 114:333–353

[11] Ratering S, Schnell S. 2000. Localization of iron-reducing activity in paddy soilby profile studies. *Biogeochemistry* 48:341–365

[12] Grigg ARC, ThomasArrigo LK, Schulz K, Rothwell KA, Kaegi R, et al. 2022. Ferrihydrite transformations in flooded paddy soils: rates, pathways, and product spatial distributions. *Environmental Science: Processes & Impacts* 24:1867–1882

[13] Borch T, Kretzschmar R, Kappler A, Van Cappellen P, Ginder-Vogel M, et al. 2010. Biogeochemical redox processes and their impact on contaminant dynamics. *Environmental Science & Technology* 44:15–23

[14] Kappler A, Bryce C, Mansor M, Lueder U, Byrne JM, et al. 2021. An evolving view on biogeochemical cycling of iron. *Nature Reviews Microbiology* 19:360–374

[15] Castenson KL, Rabenhorst MC. 2006. Indicator of reduction in soil (IRIS): evaluation of a new approach for assessing reduced conditions in soil. *Soil Science Society of America Journal* 70:1222–1226

[16] Cornell RM, Schwertmann U. 2003. Chapter 14 Transformations. In *The Iron Oxides: Structure, Properties, Reactions, Occurrences and Uses*. Germany: Wiley-VCH Verlag GmbH & Co. KGaA. pp. 365–407 doi: 10.1002/3527602097.ch14

[17] Minasny B, Malone BP, McBratney AB, Angers DA, Arrouays D, et al. 2017. Soil carbon 4 per mille. *Geoderma* 292:59–86

[18] Guo Y, Zhang S, Gustave W, Liu H, Cai Y, et al. 2024. Dynamics of cadmium and arsenic at the capillary fringe of paddy soils: a microcosm study based on high-resolution porewater analysis. *Soil & Environmental Health* 2:100057

[19] Pan Y, Bonten LTC, Koopmans GF, Song J, Luo Y, et al. 2016. Solubility of trace metals in two contaminated paddy soils exposed to alternating flooding and drainage. *Geoderma* 261:59–69

[20] Barczok M, Smith C, Di Domenico N, Kinsman-Costello L, Herndon E. 2023. Variability in soil redox response to seasonal flooding in a vernal pond. *Frontiers in Environmental Science* 11:1114814

[21] Yang D, Du T, Yang C, Yang G, Wang F, et al. 2023. Profound impact of water management on cadmium and arsenic accumulation in ratoon rice. *Field Crops Research* 302:109071

[22] Maguffin SC, Abu-Ali L, Tappero RV, Pena J, Rohila JS, et al. 2020. Influence of manganese abundances on iron and arsenic solubility in rice paddy soils. *Geochimica et Cosmochimica Acta* 276:50–69

[23] Wu J, Huang Y, Dong M, Ma H, Hu Y, et al. 2026. Iron–nitrogen synergistic mechanisms governing arsenic speciation and mobility: a critical review of interfacial reactions and microbial redox transformations. *Biogeochemistry* 169:26

[24] Somenahally AC, Hollister EB, Yan W, Gentry TJ, Loeppert RH. 2011. Water management impacts on arsenic speciation and iron-reducing bacteria in contrasting rice-rhizosphere compartments. *Environmental Science & Technology* 45:8328–8335

[25] Di Bonito M, Breward N, Crout N, Smith B, Young S. 2008. Chapter ten – overview of selected soil pore water extraction methods for the

determination of potentially toxic elements in contaminated soils: operational and technical aspects. In *Environmental Geochemistry*, eds. De Vivo B, Belkin HE, Lima A. Amsterdam: Elsevier Science. pp. 213–249 doi: 10.1016/B978-0-444-53159-9.00010-3

[26] Zhang S, Yuan Z, Cai Y, Liu H, Liu Z, et al. 2023. Dissolved solute sampling across an oxic-anoxic soil-water interface using microdialysis profilers. *Journal of Visualized Experiments* 193:e64358

[27] Garnier JM, Garnier J, Jézéquel D, Angeletti B. 2015. Using DET and DGT probes (ferrihydrite and titanium dioxide) to investigate arsenic concentrations in soil porewater of an arsenic-contaminated paddy field in Bangladesh. *Science of the Total Environment* 536:306–315

[28] Santner J, Larsen M, Kreuzeder A, Glud RN. 2015. Two decades of chemical imaging of solutes in sediments and soils – a review. *Analytica Chimica Acta* 878:9–42

[29] Jang A, Lee JH, Bhadri PR, Kumar SA, Timmons W, et al. 2005. Miniaturized redox potential probe for in situ environmental monitoring. *Environmental Science & Technology* 39:6191–6197

[30] Larsen M, Santner J, Oburger E, Wenzel WW, Glud RN. 2015. O_2 dynamics in the rhizosphere of young rice plants (*Oryza sativa* L.) as studied by planar optodes. *Plant and Soil* 390:279–292

[31] Miele F, Benettin P, Wang S, Retti I, Asadollahi M, et al. 2023. Spatially explicit linkages between redox potential cycles and soil moisture fluctuations. *Water Resources Research* 59:e2022WR032328

[32] Evans AE, Limmer MA, Seyfferth AL. 2021. Indicator of redox in soil (IRIS) films as a water management tool for rice farmers. *Journal of Environmental Management* 294:112920

[33] Castañeda C, Rodríguez-Ochoa R, Olarieta JR, Medina E, Latorre B, et al. 2024. Redox conditions and indicator of reduction in soils (IRIS) films in soils of a hypersaline wetland. *Catena* 247:108552

[34] Rabenhorst MC, Wyss-Gallifent J, Kim JD, Park CE, Wessel BM. 2025. Advances in technology for using Indicator of reduction in soils (IRIS) to quantify porewater sulfide levels in the coastal zone. *Soil Science Society of America Journal* 89:e70035

[35] Bridgham SD, Faulkner SP, Richardson CJ. 1991. Steel rod oxidation as a hydrologic indicator in wetland soils. *Soil Science Society of America Journal* 55:856–862

[36] Bwire D, Saito H, Sidle RC, Nishiwaki J. 2024. Water management and hydrological characteristics of paddy-rice fields under alternate wetting and drying irrigation practice as climate smart practice: a review. *Agronomy* 14:1421

[37] Achtnich C, Bak F, Conrad R. 1995. Competition for electron donors among nitrate reducers, ferric iron reducers, sulfate reducers, and methanogens in anoxic paddy soil. *Biology and Fertility of Soils* 19:65–72

[38] Lovley DR, Phillips EJP. 1987. Competitive mechanisms for inhibition of sulfate reduction and methane production in the zone of ferric iron reduction in sediments. *Applied and Environmental Microbiology* 53:2636–2641

[39] Thamdrup B. 2000. Bacterial manganese and iron reduction in aquatic sediments. In *Advances in Microbial Ecology*. ed. Schink B. Vol. 16. New York, NY: Springer. pp. 41–84 doi: 10.1007/978-1-4615-4187-5_2

[40] Roden EE, Wetzel RG. 1996. Organic carbon oxidation and suppression of methane production by microbial Fe(III) oxide reduction in vegetated and unvegetated freshwater wetland sediments. *Limnology and Oceanography* 41:1733–1748

[41] Hori T, Müller A, Igarashi Y, Conrad R, Friedrich MW. 2010. Identification of iron-reducing microorganisms in anoxic rice paddy soil by ^{13}C-acetate probing. *The ISME Journal* 4:267–278

[42] Kong S, Cai D, Shao Y, Wei X, Yi Z, et al. 2024. Identification of key factors and mechanism determining arsenic mobilization in paddy soil-porewater-rice system. *Journal of Hazardous Materials* 479:135684

[43] Hong Z, Xia Z, Ru Y, Chen G, Zeng RJ, et al. 2026. Key roles of iron (oxyhydr)oxides and organic matter in controlling the mobility of Ni, Cr, and Pb in redox-fluctuating basalt-derived paddy soils. *Journal of Agricultural and Food Chemistry* 74:5065–5077

[44] Galgo SJC, Canatoy RC, Lim JY, Park HC, Kim PJ. 2024. A potential of iron slag-based soil amendment as a suppressor of greenhouse gas (CH_4 and N_2O) emissions in rice paddy. *Frontiers in Environmental Science* 12:1290969

[45] Sun Z, Li H, Hu J, Wu X, Su R, et al. 2023. Fe(III) stabilizing soil organic matter and reducing methane emissions in paddy fields under varying flooding conditions. *Ecotoxicology and Environmental Safety* 259:114999

[46] Yu L, Jia R, Liu S, Li S, Shen Y, et al. 2025. Rice root iron plaque as a mediator to stimulate methanotrophic nitrogen fixation. *Environmental Science & Technology* 59:20411–20420

[47] Qiu Z, Hu M, Chen B, Long Y, Senoo K, et al. 2026. Iron amendment decreases methane emissions from subtropical paddies by altering soil microbial communities. *Microbiology Spectrum* 14:e04000-25

[48] Minamikawa K, Tokida T, Sudo S, Padre A, Yagi K. 2015. Guidelines for measuring CH_4 and N_2O emissions from rice paddies by a manually operated closed chamber method. Tsukuba, Japan: National Institute for Agro-Environmental Sciences. https://globalresearchalliance.org/wp-content/uploads/2018/02/Guidelines-for-Measuring-CH4-and-N2O-Emissions-from-Rice-Paddies-by-Manually-Operated-Closed-Chamber-Method-2015.pdf

[49] United States Department of Agriculture (USDA), Natural Resources Conservation Service (NRCS). 2026. Field indicators of hydric soils in the United States: a guide for identifying and delineating hydric soils, Version 9.3. USDA, NRCS, USA. www.nrcs.usda.gov/sites/default/files/2026-03/Field-Indicators-of-Hydric-Soils-in-the-United-States-Version-9.3.pdf

[50] Vela IY, Jensen PE, Nebel L, Kelstrup PH. 2025. Method and system for soil and groundwater *in situ* redox potential (Eh) logging. *ACS ES&T Water* 5:1075–1085

[51] Husson O. 2013. Redox potential (Eh) and pH as drivers of soil/plant/microorganism systems: a transdisciplinary overview pointing to integrative opportunities for agronomy. *Plant and Soil* 362:389–417

[52] Grenthe I, Stumm W, Laaksuharju M, Nilsson AC, Wikberg P. 1992. Redox potentials and redox reactions in deep groundwater systems. *Chemical Geology* 98:131–150

[53] Jardim WF. 2014. Medição e interpretação de valores do potencial redox (Eh) em matrizes ambientais [Measurement and interpretation of redox potential values (Eh) in environmental matrices]. *Química Nova* 37:1233–1235 (in Portuguese)

[54] Usui Y. 2013. A review of improvements to methods for the measurement of dissolved oxygen, pH, and soil redox potential and the discovery of convective flow in ponded water of paddy fields. *Climate in Biosphere* 13:25–32

[55] Pasquier V, Fike DA, Révillon S, Halevy I. 2022. A global reassessment of the controls on iron speciation in modern sediments and sedimentary rocks: a dominant role for diagenesis. *Geochimica et Cosmochimica Acta* 335:211–230

[56] Wang X, Zhang J, Yang B, Mao H, Yu Q, et al. 2025. Intermittent microaeration enhanced anaerobic digestion: the key role of Fe(III)/Fe(II) cycle and reactive oxygen species. *Environmental Science & Technology* 59:8629–8639

[57] Arpadjan S, Tsekova K, Petrova P, Knutsson J. 2012. Field sampling, speciation and determination of dissolved iron (II) and iron (III) in waters. *Bulgarian Chemical Communications* 44:299–306

[58] Köhler I, Piatka D, Barth JAC, Martinez RE. 2021. Beware of effects on isotopes of dissolved oxygen during storage of natural iron-rich water samples: a technical note. *Rapid Communications in Mass Spectrometry* 35:e9024

[59] Stumm W, Lee GF. 1961. Oxygenation of ferrous iron. *Industrial & Engineering Chemistry* 53:143–146

[60] Sung W, Morgan JJ. 1980. Kinetics and product of ferrous iron oxygenation in aqueous systems. *Environmental Science & Technology* 14:561–568

[61] Millero FJ, Sotolongo S, Izaguirre M. 1987. The oxidation kinetics of Fe(II) in seawater. *Geochimica et Cosmochimica Acta* 51:793–801

[62] Morgan B, Lahav O. 2007. The effect of pH on the kinetics of spontaneous Fe(II) oxidation by O_2 in aqueous solution – basic principles and a simple heuristic description. *Chemosphere* 68:2080–2084
[63] Roberts LC, Hug SJ, Voegelin A, Dittmar J, Kretzschmar R, et al. 2011. Arsenic dynamics in porewater of an intermittently irrigated paddy field in Bangladesh. *Environmental Science & Technology* 45:971–976
[64] Burton ED, Johnston SG, Kocar BD. 2014. Arsenic mobility during flooding of contaminated soil: the effect of microbial sulfate reduction. *Environmental Science & Technology* 48:13660–13667
[65] Fang W, Williams PN, Fang X, Amoah-Antwi C, Yin D, et al. 2018. Field-scale heterogeneity and geochemical regulation of arsenic, iron, lead, and sulfur bioavailability in paddy soil. *Environmental Science & Technology* 52:12098–12107
[66] Takahashi Y, Minamikawa R, Hattori KH, Kurishima K, Kihou N, et al. 2004. Arsenic behavior in paddy fields during the cycle of flooded and non-flooded periods. *Environmental Science & Technology* 38:1038–1044
[67] Dittmar J, Voegelin A, Roberts LC, Hug SJ, Saha GC, et al. 2010. Arsenic accumulation in a paddy field in Bangladesh: seasonal dynamics and trends over a three-year monitoring period. *Environmental Science & Technology* 44:2925–2931
[68] Kuma K, Nishioka J, Matsunaga K. 1996. Controls on iron(III) hydroxide solubility in seawater: the influence of pH and natural organic chelators. *Limnology and Oceanography* 41:396–407
[69] Stefánsson A. 2007. Iron(III) hydrolysis and solubility at 25 °C. *Environmental Science & Technology* 41:6117–6123
[70] Liu X, Millero FJ. 1999. The solubility of iron hydroxide in sodium chloride solutions. *Geochimica et Cosmochimica Acta* 63:3487–3497
[71] Liu X, Millero FJ. 2002. The solubility of iron in seawater. *Marine Chemistry* 77:43–54
[72] Ponnamperuma FN. 1972. The chemistry of submerged soils. In *Advances in Agronomy*. Amsterdam: Elsevier. pp.29–96 doi: 10.1016/S0065-2113(08)60633-1
[73] Takai Y, Kamura T. 1966. The mechanism of reduction in waterlogged paddy soil. *Folia Microbiologica* 11:304–313
[74] Van Cappellen P, Wang Y. 1996. Cycling of iron and manganese in surface sediments; a general theory for the coupled transport and reaction of carbon, oxygen, nitrogen, sulfur, iron, and manganese. *American Journal of Science* 296:197–243
[75] Weber FA, Hofacker AF, Voegelin A, Kretzschmar R. 2010. Temperature dependence and coupling of iron and arsenic reduction and release during flooding of a contaminated soil. *Environmental Science & Technology* 44:116–122
[76] Masscheleyn PH, Delaune RD, Patrick WH Jr. 1991. Effect of redox potential and pH on arsenic speciation and solubility in a contaminated soil. *Environmental Science & Technology* 25:1414–1419
[77] Islam FS, Gault AG, Boothman C, Polya DA, Charnock JM, et al. 2004. Role of metal-reducing bacteria in arsenic release from Bengal delta sediments. *Nature* 430:68–71
[78] Kocar BD, Fendorf S. 2009. Thermodynamic constraints on reductive reactions influencing the biogeochemistry of arsenic in soils and sediments. *Environmental Science & Technology* 43:4871–4877
[79] Stuckey JW, Schaefer MV, Kocar BD, Benner SG, Fendorf S. 2016. Arsenic release metabolically limited to permanently water-saturated soil in Mekong Delta. *Nature Geoscience* 9:70–76
[80] Yamaguchi N, Nakamura T, Dong D, Takahashi Y, Amachi S, et al. 2011. Arsenic release from flooded paddy soils is influenced by speciation, Eh, pH, and iron dissolution. *Chemosphere* 83:925–932
[81] Yin DX, Fang W, Guan DX, Williams PN, Moreno-Jimenez E, et al. 2020. Localized intensification of arsenic release within the emergent rice rhizosphere. *Environmental Science & Technology* 54:3138–3147
[82] Cai X, Yin N, Liu X, Wang P, Du H, et al. 2022. Biogeochemical processes of arsenic transformation and redistribution in contaminated soils: combined effects of iron, sulfur, and organic matter. *Geoderma* 422:115948
[83] Xu X, Wang P, Zhang J, Chen C, Wang Z, et al. 2019. Microbial sulfate reduction decreases arsenic mobilization in flooded paddy soils with high potential for microbial Fe reduction. *Environmental Pollution* 251:952–960
[84] Yuan ZF, Gustave W, Bridge J, Liang Y, Sekar R, et al. 2019. Tracing the dynamic changes of element profiles by novel soil porewater samplers with ultralow disturbance to soil–water interface. *Environmental Science & Technology* 53:5124–5132
[85] Zhao FJ, McGrath SP, Meharg AA. 2010. Arsenic as a food chain contaminant: mechanisms of plant uptake and metabolism and mitigation strategies. *Annual Review of Plant Biology* 61:535–559
[86] Boudreau BP. 1997. *Diagenetic Models and Their Implementation*. Berlin: Springer.
[87] Postma D, Larsen F, Minh Hue NT, Duc MT, Viet PH, et al. 2007. Arsenic in groundwater of the Red River floodplain, Vietnam: controlling geochemical processes and reactive transport modeling. *Geochimica et Cosmochimica Acta* 71:5054–5071
[88] Wang Z, Liu X, Liang X, Dai L, Li Z, et al. 2022. Flooding-drainage regulate the availability and mobility process of Fe, Mn, Cd, and as at paddy soil. *Science of the Total Environment* 817:152898
[89] Sander M, Hofstetter TB, Gorski CA. 2015. Electrochemical analyses of redox-active iron minerals: a review of nonmediated and mediated approaches. *Environmental Science & Technology* 49:5862–5878
[90] Pentráková L, Su K, Pentrák M, Stucki JW. 2013. A review of microbial redox interactions with structural Fe in clay minerals. *Clay Minerals* 48:543–560
[91] Davison W. 1991. The solubility of iron sulphides in synthetic and natural waters at ambient temperature. *Aquatic Sciences* 53:309–329
[92] Rickard D, Luther GW. 2007. Chemistry of iron sulfides. *Chemical Reviews* 107:514–562
[93] Barreto MSC, Hurtarte LCC, Nehzati S, Izaditame F, LeMonte JJ, et al. 2025. Impact of geochemical iron and sulfur redox cycling on arsenic release along a salinity gradient: Sea level rise implications. *Journal of Hazardous Materials* 499:140071
[94] Couture RM, Charlet L, Markelova E, Madé B, Parsons CT. 2015. On-off mobilization of contaminants in soils during redox oscillations. *Environmental Science & Technology* 49:3015–3023
[95] Fujii M, Imaoka A, Yoshimura C, Waite TD. 2014. Effects of molecular composition of natural organic matter on ferric iron complexation at circumneutral pH. *Environmental Science & Technology* 48:4414–4424
[96] Singer PC, Stumm W. 1970. Acidic mine drainage: the rate-determining step. *Science* 167:1121–1123
[97] Stockdale A, Davison W, Zhang H. 2009. Micro-scale biogeochemical heterogeneity in sediments: a review of available technology and observed evidence. *Earth-Science Reviews* 92:81–97
[98] Brune A, Frenzel P, Cypionka H. 2000. Life at the oxic–anoxic interface: microbial activities and adaptations. *FEMS Microbiology Reviews* 24:691–710
[99] Liu HB, Sun HX, Du LQ, Jiang LL, Zhang LA, et al. 2024. Rice receptor kinase FLR7 regulates rhizosphere oxygen levels and enriches the dominant *Anaeromyxobacter* that improves submergence tolerance in rice. *The ISME Journal* 18:wrae006
[100] Li XY, Li SQ, Jiang YF, Yang Q, Zhang JC, et al. 2024. Multi-imaging platform for rhizosphere studies: Phosphorus and oxygen fluxes. *Journal of Environmental Management* 351:119763
[101] Luther GW, Rickard DT, Theberge S, Olroyd A. 1996. Determination of metal (Bi)sulfide stability constants of Mn^{2+}, Fe^{2+}, Co^{2+}, Ni^{2+}, Cu^{2+}, and Zn^{2+} by voltammetric methods. *Environmental Science & Technology* 30:671–679
[102] Mehla MK, Singh A, Jeong J, Ran L. 2026. Global methane emissions from rice paddies are now increasingly quantifiable. *Communications Earth & Environment* 7:643

Copyright: © 2026 by the author(s). Published by Maximum Academic Press, Fayetteville, GA. This article is an open access article distributed under Creative Commons Attribution License (CC BY 4.0), visit https://creativecommons.org/licenses/by/4.0/.